Polymer Brushes by Living Anionic Surface Initiated Polymerization on Flat Silicon (SiOx) and Gold Surfaces: Homopolymers and Block Copolymers

ARTICLE *in* LANGMUIR · JANUARY 2002

Impact Factor: 4.46

CITATIONS
4

READS
9

1 AUTHOR:

Georgios Sakellariou
National and Kapodistrian University of Athens
58 PUBLICATIONS **608** CITATIONS

SEE PROFILE

Polymer Brushes by Living Anionic Surface Initiated Polymerization on Flat Silicon (SiO_x) and Gold Surfaces: Homopolymers and Block Copolymers

Rigoberto Advincula,*[,†,‡] Qingye Zhou,[†] Mikyoung Park,[†] Shuangxi Wang,[†] Jimmy Mays,[†,§] George Sakellariou,[||] Stergios Pispas,[||] and Nikos Hadjichristidis[||]

Department of Chemistry, University of Alabama at Birmingham, Birmingham, Alabama 35294, Department of Chemistry, University of Houston, Houston, Texas 77204, Department of Chemistry, University of Tennessee, Knoxville, Tennessee 37996-1600 and Oak Ridge National Laboratory, Oak Ridge, Tennessee, and Department of Chemistry, University of Athens, 15701 Zografou, Athens, Greece

Received May 17, 2002. In Final Form: August 2, 2002

The formation of homopolymer and block copolymer brushes grafted from Au and Si (SiO_x) surfaces via living anionic surface-initiated polymerization (LASIP) is described. The initiator precursor 1,1-diphenylethylene (DPE) was functionalized with alkylsilane or alkylthiol and grafted onto planar Si wafer and Au surfaces, respectively, by self-assembled monolayer techniques. *n*-BuLi was used to activate the DPE initiator for anionic polymerization of monomers at the interface. A high-vacuum reactor was used for polymerization at surfaces under anhydrous solution conditions. By a careful sequence of monomer introduction, reaction, and termination, homopolymer and block copolymer tethered polymer brushes were obtained. The grafted polymer chains were investigated using surface sensitive techniques such as ellipsometry, contact angle measurements, atomic force microscopy, Fourier transform infrared spectroscopy, surface plasmon spectroscopy, and X-ray photoelectron spectroscopy. The importance of activation of the grafted initiator, control of polymerization conditions, and removal of excess BuLi is emphasized. Interesting differences in morphology, thickness, grafting density, and polymerization conditions contrast LASIP from solution and other surface-initiated polymerization mechanisms. The formation of block copolymer sequences highlights the unique utility of a living anionic polymerization technique on surfaces.

Introduction

Polymer brushes on solid surfaces are of great interest for surface modification and composite material preparation.[1−3] A number of model surface grafting techniques have been used on planar surfaces and particles. One of the most reported methods involves physical adsorption or physisorption of functionalized homopolymers or block copolymers.[4] However, such adsorbed layers are susceptible to removal, for example, by exposure to a thermodynamically good solvent. It is often difficult to control the physical structure and density of such adsorbed layers from both entropic and enthalpic considerations. In principle, adhesion between the polymer and the substrate may be greatly enhanced if the chains are chemically adsorbed or chemisorbed onto surfaces covalently. This approach involves reaction of end-functionalized polymers with reactive sites on a substrate surface.[5] The disadvantage of this grafting method is that chain ends have to first find their way to the surface and react. Furthermore, polymer chains attached at the beginning of the reaction sterically shield the remaining surface reactive sites such that brush density becomes self-limiting.[6] Thus, both physisorption and chemisorption have their drawbacks for grafting onto surfaces. In this respect, grafting from surfaces by surface-initiated polymerization (SIP) has important advantages in terms of polymer brush densities and other physical properties. SIP promotes polymerization of monomers directly from initiator sites already attached to surfaces, in which case, activation of the initiator and diffusion of monomers to the reactive sites become the primary factors.[7] Furthermore, it is possible to prepare grafted polymers for which the average distance between grafting points is much smaller than the radius of gyration (Rg). Thus, this latter approach appears to be more promising and versatile for preparing tethered "polymer brushes".

The SIP approach to polymer brushes has been of great interest in recent years.[8] They can be prepared by a number of polymerization mechanisms including free-radical[7] or cationic[9] polymerization, ring-opening metathesis polymerization (ROMP),[10] atom transfer free-radical polymerization (ATRP),[11] polymerizations using 2,2,6,6-tetramethyl-1-piperidyloxy (TEMPO),[12] and anionic polymerization.[13] All these methods are suitable for polymerizing different types of monomers on a variety of

[†] University of Alabama at Birmingham.
[‡] University of Houston.
[§] University of Tennessee and Oak Ridge National Laboratory.
[||] University of Athens.

(1) Halperin, A.; Tirrell, M.; Lodge, T. P. *Adv. Polym. Sci.* **1992**, *100*, 31.
(2) Tadros, T. *The Effect of Polymers on Dispersion Properties*; Academic Press: London, 1982.
(3) Krishnamoorti, R.; Vaia, R. *Polymer Nanocomposites*; ACS Symposium Series 804; American Chemical Society: Washington, DC, 2002.
(4) Fleer, G. J.; Cohen-Stuart, M. A.; Scheutjens, J. M. H. M.; Cosgrove, T.; Vincent, B. *Polymers at Interfaces*; Chapman & Hall: London, 1993.
(5) (a) Al-Maawali, S.; Bemis, J.; Akhremitchev, B.; Leecharoen, R.; Janesko, B.; Walker, G. *J. Phys. Chem. B* **2001**, *105*, 3965. (b) Jordan, R.; Graf, K.; Riegler, H.; Unger, K. K. *Chem. Commun.* **1996**, *9*, 1025. (c) Zhao, W.; Krausch, G.; Rafailovich, M. H.; Sokolov, J. *Macromolecules* **1994**, *27*, 2933.
(6) Balazs, A.; Lyatskaya, Y. *Macromolecules* **1998**, *31*, 6676.
(7) Prücker, O.; Rühe, J. *Langmuir* **1998**, *14*, 6893.
(8) Zhao, B.; Brittain, W. *Prog. Polym. Sci.* **2000**, *25*, 677.
(9) Jordan, R.; Ulman, A. *J. Am. Chem. Soc.* **1998**, *120*, 243.
(10) Weck, M.; Jackiw, J.; Rossi, R.; Weiss, P.; Grubbs, R. *J. Am. Chem. Soc.* **1999**, *121*, 4088.

10.1021/la025962t CCC: $22.00
Published on Web 09/27/2002

flat surfaces and particles. More recently, a number of innovative analytical tools for both particle and surface analysis have allowed elucidation of polymerization mechanism and physical properties of these tethered polymers.

Among the polymerization techniques mentioned above, a living anionic polymerization should show the best possible control of polymer architecture. Monodisperse homopolymers and complex block, graft, star, and miktoarm architectures have been accessible primarily by anionic polymerization methods.[14] This method has been used to grow polymer brushes from various small particles such as silica gels,[15] graphite and carbon black,[16] and also flat surfaces.[13,17−19] We have recently reported our results on living anionic polymerization on clay[20] and Si nanoparticles.[21] Difficulties arise due to effects of moisture and other impurities on anionic polymerization, especially with polymerization from clay surfaces. Other problems can also be present. For example, a major limitation of previous work is the use of *tert*-butyllithium (*t*-BuLi) as an initiator for styrene SIP in toluene.[15] *t*-BuLi initiation is very slow in nonpolar solvents, yielding broad molecular weight (MW) distributions and higher than expected MWs.[22] In the previous work, a 6-fold excess of *t*-BuLi was used and it was assumed that the molecular weights of grafted and nongrafted polymer were the same. The researchers were not able to investigate differences between free polymerization in solution and confined polymerization on surfaces. Despite these difficulties, anionic polymerization remains attractive for the synthesis of complex and well-defined macromolecular architectures.[14]

Although polymerization on particle surfaces[23] is one of the best ways of obtaining more polymer samples for analysis (because of the high surface-to-volume ratio), polymerization on flat surfaces has advantages primarily of availability of surface sensitive analytical techniques. Also, there is potential for polymer brush applications in surface modification and patterning.[24] Theoretical predictions have been used to calculate MW and polydispersity of polymer brushes grown by SIP on flat surfaces.[25] Other theoretical predictions have been made on conformation and dynamic behavior of tethered polymers at surfaces.[26] It will be interesting to verify theoretical predictions on block copolymer brush behavior with respect to the Flory−Huggins (χ) interaction parameter, Kuhn length, block volume fraction, and substrate surface energies.[27] Interesting mesophases of block copolymer brushes on surfaces have been predicted based on a variety of surface interactions.[28] Thus, the development of techniques for the synthesis of tethered homopolymer and block copolymer brushes should be carefully explored.[8]

This paper describes our detailed investigation on covalently attached homopolymers and block copolymers on flat Au and Si (SiO_x) surfaces by living anionic surface-initiated polymerization (LASIP). To investigate living anionic polymerization on surfaces, we have utilized 1,1-diphenylethylene (DPE) with chlorosilane and thiol end-groups as an initiator precursor tethered by the self-assembled monolayer (SAM) technique. The DPE group is an efficient initiator for anionic polymerization after activation with BuLi. It avoids the potential for "two-dimensional polymerization" on the surface since DPE cannot propagate by itself. Using a high-vacuum reactor, anionic polymerization was achieved forming homopolymers and block copolymers "grafted from" the surface. The composition, thickness, physical and thermal properties, and morphology of the tethered polymer brushes were analyzed. A variety of surface sensitive techniques such as ellipsometry, contact angle measurements, atomic force microscopy (AFM), quartz crystal microbalance (QCM), Fourier transform infrared (FT-IR) grazing incidence and polarization modulation infrared reflection−absorption spectroscopy (PM-IRRAS), surface plasmon spectroscopy (SPS), and X-ray photoelectron spectroscopy (XPS) were utilized. Interesting insights on the living anionic polymerization phenomena and mechanism on flat surfaces were obtained.

Experimental Section

Materials. Benzene (Fisher, >99%), tetrahydrofuran or THF (Aldrich, 99.9%), and hexane (Aldrich, 99.9%) were purified according to anionic polymerization solvent standards, as described in the literature.[29] Styrene (Aldrich, 99%) was stirred with CaH_2 overnight at room temperature and degassed three times on the vacuum line. The "roughly" purified styrene was treated with dibutylmagnesium ($MgBu_2$, Aldrich, 1.0 M in heptane) for a few hours and then finally distilled into ampules. Other monomers (isoprene and butadiene) were likewise purified using standard purification techniques suitable for anionic polymerization.[29,30] *n*-Butyllithium (*n*-BuLi) was freshly prepared by reacting 1-chlorobutane with Li powder in hexane under a vacuum. Methanol was treated with CaH_2 overnight and degassed three times on the vacuum line before distillation into ampules.

Characterization. A Bruker ARX-300 proton nuclear magnetic resonance (^{1}H NMR) instrument was used to obtain ^{1}H NMR and ^{13}C NMR spectra in $CDCl_3$. A QCM, Maxtek Inc., with a phase-locked PLO-10 oscillator and PM-740 frequency counter was used to measure the mass and density of the DPE initiator.

(11) (a) Ejaz, M.; Yamamoto, S.; Ohno, K.; Tsujii, Y.; Fukuda, T. *Macromolecules* **1998**, *31*, 5934. (b) Kong, X.; Kawai, T.; Abe, J.; Iyoda, T. *Macromolecules* **2001**, *34*, 1837. (c) Yamamoto, S.; Tsujii, Y.; Fukuda, T. *Macromolecules* **2000**, *33*, 5995. (d) von Werne, T.; Patten, T. *J. Am. Chem. Soc.* **2001**, *123*, 7497. (e) Jones, D.; Brown, A.; Huck, W. *Langmuir* **2002**, *18*, 1265.

(12) Husseman, M.; Malmstrom, E.; McNamara, M.; Mate, M.; Mecereyes, D.; Genoit, d. G.; Hedrick, J.; Mansky, P.; Huang, E.; Russell, T.; Hawker, C. *Macromolecules* **1999**, *32*, 1424.

(13) Zhou, Q.; Nakamura, Y.; Inaoka, S.; Park, M.; Wang, Y.; Mays, J.; Advincula, R. *Polym. Mater. Sci. Eng. Prepr.* (*Am. Chem. Soc.*) **2000**, *82*, 291.

(14) Pitsikalis, M.; Pispas, S.; Mays, J.; Hadjichristidis, N. *Adv. Polym. Sci.* **1998**, *135*, 1.

(15) Oosterling, M.; Sein, A.; Schouten, A. *Polymer* **1992**, *33*, 4394.

(16) Tsubokawa, N.; Yoshihara, T.; Sone, Y. *Colloid Polym. Sci.* **1991**, *269*, 324.

(17) Zhou, Q.; Wang, S.; Fan, X.; Pispas, S.; Sakellariou, G.; Hadjichristides, N.; Mays, J.; Advincula, R. *Polym. Prepr.* (*Am. Chem. Soc., Div. Polym. Chem.*) **2001**, *42*, 59.

(18) (a) Quirk R.; Mathers, R. *Polym. Bull.* **2001**, *6*, 471. (b) Ingall, M.; Honeyman, C.; Mercure, J.; Bianconi, P.; Kunz, R. *J. Am. Chem. Soc.* **1999**, *121*, 3607.

(19) Jordan, R.; Ulman, A.; Kang, J.; Rafailovich, M.; Sokolov, J. *J. Am. Chem. Soc.* **1999**, *121*, 1016.

(20) Zhou, Q.; Fan, X.; Xia, C.; Mays, J.; Advincula, R. *Chem. Mater.* **2001**, *13*, 2465.

(21) Zhou, Q.; Wang, S.; Fan, X.; Advincula, R.; Mays, J. *Langmuir* **2002**, *18*, 3324.

(22) Morton, M.; Fetters, L. *J. Rubber Chem. Technol.* **1975**, *48*, 359.

(23) Prücker, O.; Rühe, J. *Macromolecules* **1998**, *31*, 592.

(24) Husemann, M.; Morrison, M.; Benoit, D.; Frommer, J.; Mate, M.; Hinsberg, W.; Hedrick, J.; Hawker, C. *J. Am. Chem. Soc.* **2000**, *122*, 1844.

(25) (a) Milner, S. T. *Science* **1991**, *252*, 905. (b) Milner, S. T.; Witten, T. A.; Cates, M. E. *Macromolecules* **1988**, *21*, 2610. (c) Minko, S.; Gafijchuk, G.; Sidorenko, A.; Voronov, S. *Macromolecules* **1999**, *32*, 4525.

(26) Alexander, S. *J. Phys.* **1977**, *38*, 977.

(27) (a) Rockford, L.; Mochrie, S.; Russell, T. *Macromolecules* **2001**, *34*, 1487. (b) Russell, T.; Thurn-Albrecht, T.; Tuominen, M.; Huang, E.; Hawker, C. *Macromol. Symp.* **2000**, *159*, 77. (c) Rockford, L.; Liu, Y.; Mansky, P.; Russell, T.; Yoon, M.; Mochrie, S. *J. Phys. Rev. Lett.* **1999**, *82*, 2602. (d) Zhulina, E. B.; Balzs, A. C. *Macromolecules* **1996**, *29*, 6338.

(28) (a) Fasolka, M.; Banerjee, P.; Mayes, A.; Pickett, G.; Balazs, A. *Macromolecules* **2000**, *33*, 5702. (b) Pereira, G.; Williams, D. *Macromolecules* **1999**, *32*, 758.

(29) Förster, S.; Krämer, E. *Macromolecules* **1999**, *32*, 2783.

(30) Hadjichristidis, N.; Iatrou, H.; Pispas, S.; Pitsikalis, M. *J. Polym. Sci., Part A: Polym. Chem.* **2000**, *38*, 3211.

Scheme 1. Synthesis of the Silane−DPE Initiator Using Grignard Coupling and Hydrosilylation

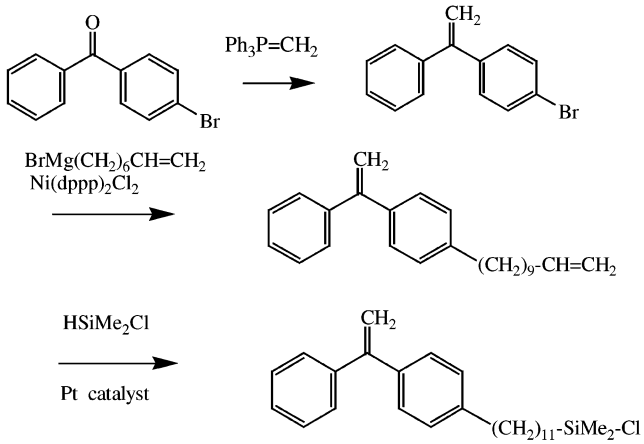

Scheme 2. Synthesis Scheme for the Thiol−DPE Initiator

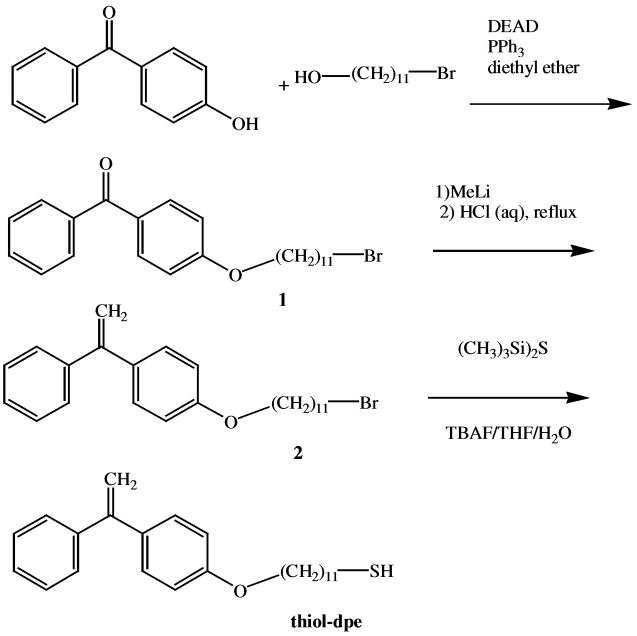

The quartz crystal electrode was modified by SAM formation for the initiator. Ellipsometric thickness measurements were performed using the Multiskop ellipsometer (Optrel GmbH, Germany) with a 632.8 nm He−Ne laser beam as the light source at a 70° angle of incidence. Both delta and psi values (thickness data) were measured and calculated using integrated specialized software that came with the instrument. The surface plasmon spectra were measured using the SPS mode of the Multiskop with a Kretschmann configuration and attenuated total reflection conditions.[31] The reflectance was monitored with a p-polarized He−Ne laser (632.8 nm) as a function of the angle of incidence. Au (486 Å) was deposited onto glass substrates with at an evaporation rate of approximately 12 Å/s. XPS was done using a Kratos Axis 165 Multitechnique Electron Spectrometer system. A monochromatic Al Kα X-ray source (1486.6 eV) operated at 15 kV and 20 mA was applied to excite the photoelectron emission at $\theta = 0$ (normal to the surface). Fixed analyzer transmission (FAT) mode was used, and survey scans (spot of 800 × 200 μm^2, resolution 4 eV at analyzer pass energy of 160 eV) were collected from 0 to 1400 eV to obtain the elemental composition of the polymer film. The C 1s peak of the hydrocarbon signal (284.5 eV) was used as binding energy reference. A built-in charge neutralizer was operated to compensate for charge buildup during the measurements. Infrared (IR) spectra were obtained using a Nicolet NEXUS 470 FT-IR system with a grazing incidence angle attachment for specular or low-angle measurements on Au-coated glass substrates (ca. 450 Å). PM-IRRAS measurements were also made with the gold-coated glass substrates. The spectra were collected using a Nicolet MAGNA-IR 860 spectrometer equipped with a liquid-nitrogen-cooled mercury−cadmium-telluride (MCT) detector and a Hinds Instruments PEM-90 photoelastic modulator (37 kHz). The light was reflected from the samples at an 80° angle and collected over 256 scans at a spectral resolution of 4 cm^{-1}. The polymer film morphologies were studied by AFM using a PicoScan system (Molecular Imaging) equipped with an 8 × 8 micron scanner. Magnetic AC (MAC) mode was used for all AFM images. A MAC lever, a silicon nitride based cantilever coated with magnetic film, was used as the AFM tip. The force constant of the tip is 0.5 N/m, and the resonance frequency is around 100 kHz. All samples were measured inside a suspension chamber to minimize ambient disturbance.

Synthesis of the Silane−DPE Initiator (Scheme 1).

The detailed synthesis procedure for the silane−DPE initiator has been reported previously.[32] In general, a Wittig reaction converts the benzophenone starting material to a brominated 1,1-diphenylethylene followed by a Grignard coupling reaction with 1,11-bromoundecene. A hydrosilylation reaction converts the product into a chlorosilane derivative. The last step affords a route to monochloro-, dichloro-, trichloro-, or other alkoxysilane end-groups, which have selective reactivities to surface hydroxyls of silicate (SiO_x) surfaces. Several of these derivatives have been recently synthesized. The initiator used for these experiments involved the monochlorosilane.

Synthesis of the Thiol−DPE Initiator (Scheme 2**). Synthesis of Compound 1**. To a solution of 4-hydroxyl benzophenone (3.96 g, 20 mmol), a mixture of 11-bromoundecane (5.0 g, 20 mmol) and triphenyl phosphine (5.24 g, 20 mmol) in 50 mL of diethyl ether diethyl azodicarboxylate (DEAD) (3.48 g, 20 mmol) was added dropwise with stirring under a N_2 atmosphere. After addition of DEAD was completed, the reaction mixture was allowed to stir overnight until a white precipitate formed. The reaction mixture was filtered to remove the precipitate, and the filtrate was collected. Removal of the solvent yielded a residue, which was purified by chromatography on silica gel using hexanes−ethyl acetate (8:1 v/v) as the eluent to give 7.65 g (yield, 89%) of the pure compound **1** as a white solid. ^{1}H NMR ($CDCl_3$): 7.70−7.35 (5H, m, Ar−H), 7.54 (2H, d, J = 8.8 Hz, Ar−H), 6.95 (2H, J = 9.0 Hz, Ar−H), 4.03 (2H, trip, J = 6.3 Hz, $-OCH_{2-}$), 3.41 (2H, trip, J = 6.6 Hz, $-CH_2Br$), 1.87−1.30 (18H, m, $-(CH_2)_{9-}$). LC−MS: 433 (M + H).

Synthesis of Compound 2. To a solution of compound **1** (4.30 g, 10 mmol) in 50 mL of dry diethyl ether was added methyllithium (1.4 M, 8 mL) in diethyl ether under a nitrogen atmosphere with stirring at room temperature. After the addition was completed, the reaction mixture was allowed to stir for an additional 6 h. The reaction mixture was then treated with 20 mL of 5 M HCl (aq), and the resultant mixture was refluxed for 3 h. The organic phase was collected, and the solvent was removed by rotary evaporation. The resultant residue was purified by chromatography on silica gel using hexanes−ethyl acetate (16:1 v/v) as the eluent to give 2.8 g (yield, 65%) of the pure compound **2** as a white solid. ^{1}H NMR ($CDCl_3$): 7.34−7.31 (5H, m, Ar−H), 7.25 (2H, d, J = 8.8, Ar−H), 6.84 (2H, J = 8.0, Ar−H), 5.39, 5.34 (2H, J = 4.5 Hz, $=CH_2$), 3.94 (2H, trip, J = 6.4 Hz, $-OCH_{2-}$), 3.40 (2H, trip, J = 6.7 Hz, $-CH_2Br$), 1.87−1.30 (18H, m, $-(CH_2)_{9-}$). LC−MS: 430 (M + H).

Synthesis of the Compound Thiol−DPE. A stirred solution of compound **2** (858 mg, 2 mmol), was cooled to −10 °C, and hexamethyldisilathiane (2.4 mol) and TBAF (tetrabutylammonium fluoride) (2.4 mL, 1.0 M solution in THF with 5% water) were added. The resultant reaction mixture was allowed to warm to room temperature while being stirred. The mixture was stirred for 2 h, diluted with a common organic solvent (methyl chloride), and washed with aqueous ammonium chloride (sat.), and the organic phase was collected. The organic solvent was removed by rotary evaporation, and the resultant residue was purified by

(31) Knoll, W. *Annu. Rev. Phys. Chem.* **1998**, *49*, 569.
(32) Zhou, Q.; Nakamura, Y.; Inaoka, S.; Park, M.; Wang, Y.; Mays, J.; Advincula, R. In *Polymer Nanocomposites*; Krishnamoorti, R., Vaia, R., Eds.; ACS Symposium Series 804; American Chemical Society: Washington, DC, 2002.

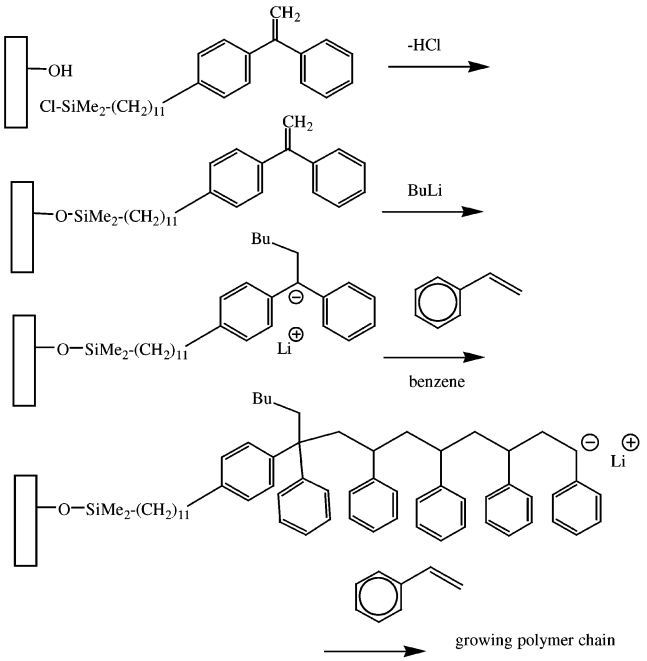

Figure 1. Immobilization of the DPE initiator followed by polymerization of the styrene homopolymer to form PS brushes by SIP.

chromatography on silica gel using hexanes−ethyl acetate (5:1 v/v) as the eluent to give 481 mg (yield, 62.9%) of the pure compound thiol−DPE as a white solid. ^{1}H NMR ($CDCl_3$): 7.34−7.30 (5H, m, Ar−H), 7.26 (2H, d, J = 8.8, Ar−H), 6.83 (2H, J = 8.0, Ar−H), 5.39, 5.34 (2H, J = 4.5 Hz, =CH_2), 3.94 (2H, trip, J = 6.4 Hz, −OCH_2−), 2.68 (2H, trip, J = 6.7 Hz, −CH_2SH), 1.87−1.30 (18H, m, −$(CH_2)_9$−). LC−MS: 383 (M + H).

Immobilization of the Initiator Precursor. The SAM of the DPE initiators was prepared as follows (as shown in Figure 1): Both Au-coated glass and Si wafer substrates were treated with plasma cleaning (under Ar, using PLASMOD, March Instruments), and the Si wafer was cleaned with an additional piranha solution (30% H_2O_2/70% H_2SO_4, 15 min) treatment. The substrates were thoroughly rinsed with Milli-Q purified H_2O and dried in an oven (90 °C) overnight before use. Modified Au-coated quartz crystals (QCM substrates) were plasma-treated under O_2 followed by argon conditions. To adsorb the silane−DPE initiators, the cleaned substrates were immersed in a 1 mM solution of the organosilane initiator in toluene (under N_2 gas) for more than 12 h. After reaction, the substrates were sonicated for 15 min with (1) toluene, (2) toluene/acetone, 1:1, and (3) acetone in sequence. The substrates were then immediately transferred to the vacuum line (under N_2 gas) and sealed. The procedure for the DPE initiator SAM formation on Au involved dipping the substrate in ethanol solutions of the initiator (10^{-4} M in ethanol for 3 h) and subsequent copious washing with ethanol. All the surfaces were characterized before and after polymerization.

Polymerization Procedure for the Homopolymer (Polystyrene or PS). The polymerization scheme is described in Figure 1. The polymerization reaction was done on a custom-made high-vacuum glass reactor apparatus similar to that shown in Figure 2. Styrene was stirred with CaH_2 overnight, degassed three times on the vacuum line, and then distilled into the flask containing dibutylmagnesium. After stirring for a few hours, it was distilled into ampules. Benzene was stirred with CaH_2 overnight, degassed three times, and then distilled into a flask with BuLi and a small amount of styrene (concentrations summarized in Table 1). After placing the DPE-SAM-coated Si wafer or Au (25 × 38 mm) in the reactor and sealing, the *s*-BuLi or *n*-BuLi (about 1×10^{-3} mol in 5 mL of hexane) was injected into the purge section through the septum. The solution was left with the substrate overnight. Excess BuLi solution was then removed, and the surface was washed several times with degassed benzene to ensure removal of excess BuLi and impurities. THF,

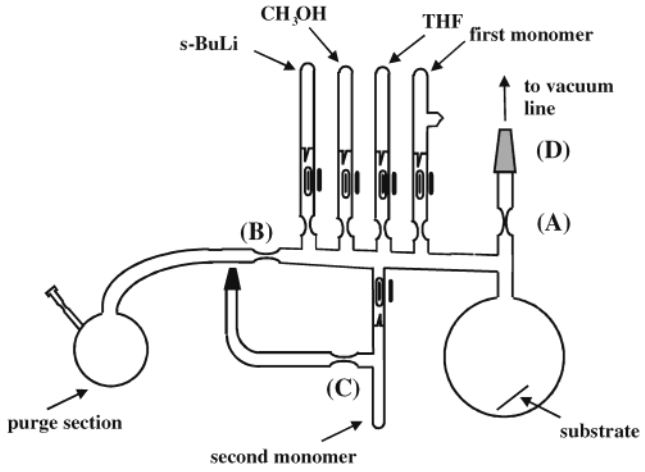

Figure 2. Polymerization setup for LASIP for preparation of homopolymer and block copolymer.

Table 1

sample (polymerization time and g styrene)[a]	activation	additive (12 mL)	thickness[b] in nm	contact angle (deg)
1 (1 day, 5.1 g)	*s*-BuLi	none	6.8	95
2 (3 days, 5.0 g)	*n*-BuLi	THF	10.8 (16%)	70
			16.1 (100%)	76
3 (5 days, 15.1 g)	*n*-BuLi	THF	13.4 (16%)	95
			13.7 (100%)	89
4 (3 days, 12.0 g)	*s*-BuLi	BuOLi	3.8 (16%)	50
			3.9 (100%)	72
5 (5 days, 12.0 g)	*n*-Buli	THF	6.3 (16%)	61
			8.2 (100%)	64
6[c,f] (3 days, 7.0 g)	*n*-BuLi	THF	8.9	82
7[c] (3 days, 2.5 g)	*n*-BuLi	THF	4.7	74
8 (5 days, 2.0 g)	*s*-BuLi	none	6.2	81
9[g] (5 days, 2.0 g)	*n*-BuLi	THF	10.1	80
10 (3 days, 2.5 g)	*s*-BuLi	THF	6.5	63
11[d] (5 days, 10.9 g)	*s*-BuLi	TMEDA	23.4[e]	94

[a] All polymerizations were done at room temperature, 24−25 °C. The volume of benzene solvent is 100 mL. Termination was done by the addition of 2 mL of methanol. [b] Brackets indicate % of DPE initiator with alkydimethylchlorosilane solution (0.0001 M) for SAMs. [c] The polymer films of samples 6 and 7 were synthesized under the drybox (inert atmosphere). [d] For PS homopolymer: 10.9 g of styrene, 1.5 mL of TMEDA, and 5×10^{-3} mol of *s*-BuLi. The substrate used was Au-coated glass. [e] Thickness obtained by surface plasmon spectroscopy. Almost no difference in thickness was observed with Soxhlet extraction (23.4) and washing procedure (22.8). [f] Free polymer from solution Mn = 1.10×10^6, PD = 1.44, by SEC. [g] Free polymer from solution Mn = 1.08×10^4, PD = 1.24, by SEC.

tetramethylethylenediamine (TMEDA), or BuOLi was also added into the initiator solution to observe its effect on the initiation of DPE. The styrene monomer was then introduced to 100 mL of freshly distilled solvent (substrate immersed) by breaking the break seal between the reactor and the monomer ampule. The polymerization was allowed to proceed for periods of a few hours to a few days before termination with MeOH (2 mL). The samples were taken out of the reactor and immediately washed using Soxhlet extraction procedures for 36 h under toluene. An alternative procedure was also used for Au substrates which involved washing at least six times with toluene, and the thickness was monitored until a constant value was obtained.

Polymerization Procedure for the Block Copolymers. The addition of initiator, reagents, and monomers was carried out similarly from the break seals using the apparatus as shown in Figure 2 under high vacuum. The detailed procedure for polystyrene-*b*-polyisoprene (PS-*b*-PI) and polybutadiene-*b*-polystyrene (PBd-*b*-PS) is as follows: After the DPE-SAM-coated substrate (Au or Si) was placed into the reactor, the apparatus was attached to the vacuum line, checked for leaks, flame-dried, and evacuated. Purified benzene (100 mL) was distilled into the

purge section frozen by liquid nitrogen and evacuated (freeze−thawing cycle). The apparatus was removed from the line by heating constriction A (Figure 2). Afterward, the *s*-BuLi solution with a small amount (2 mL) of THF was added and allowed to react with the surface-bound DPE for 8−10 h. Several careful washings with distilled benzene were done to remove excess *s*-BuLi, which was collected into the purge section and subsequently detached by heating constriction B. Thus, what is left on the apparatus is a clean glass reactor with an appropriate amount of pure solvent and monomers. The first monomer solution was poured into the reaction flask and left to react with the surface-bound living DPE anion for 1 week at room temperature. Then the whole apparatus was attached again to the vacuum line through the second ground joint (2), and the purified second monomer was distilled into the ampule. The reactor was again removed from the vacuum line by heating at constriction C, and the second monomer was poured to the reaction. The polymerization of this second block was allowed to proceed for 1 week before termination with methanol. This procedure can be considered as a general scheme for other block copolymer brush architectures.

Results and Discussion

Synthesis of the Initiator and SAM Formation. The design parameters of the initiator combine DPE functionality, spacer (alkyl chain), and reactive end-group (chlorosilane or thiol). The DPE is separated from the silyl or thiol group by an alkyl spacer. The synthesis route should allow for a homologous series of alkyl chain lengths or a variety of end-reactive groups. The former may ultimately be an important parameter for forming ideal and well-packed monolayers with much longer alkyl chains.[33] In addition, a well-packed monolayer provides a "protective layer" that may prevent reactive groups, for example, excess *n*-BuLi, from cleaving the tethered initiator from the surface. DPE was chosen to avoid self-polymerization parallel to the plane surface.[34] Activation with a nucleophile like *n*-BuLi is necessary for anionic species to form at the surface. Previously reported schemes had problems in that the surface initiators were also capable of self-polymerization.[15]

The SAM preparation was done under an inert atmosphere (drybox). For Si surfaces, a well-packed monolayer can eliminate the presence of Si−OH groups that can interfere with anionic polymerization.[35] This factor should not be a problem with Au surfaces. Ellipsometry, contact angle, AFM, SPS, and QCM were used to characterize adsorption properties of the DPE onto flat Si and Au surfaces. For the Si wafer (SiO_x surface of the wafer), the contact angle changed from 20° to 82°, indicating a change in wetting properties of the surface after chemisorption of the initiator by the SAM. AFM measurements did not indicate any distinct morphology features compared to the bare SiO_x or Au surface. For the Au surface, a frequency change of $\Delta F = -1.44$ (Hz) indicated a thickness of 1.7 nm for the DPE with a density of $\sim$1 g/cm^3 using the Sauerbrey equation.[36,37] This was verified by ellipsometric measurements with a DPE surface thickness of about 1.7 ± 2 nm. From the SPS curve (Figure 8a), it is also clear that the DPE monolayer was formed at a thickness of 1.8 ± 0.1 nm consistent with ellipsometry and QCM data. This is the thickness of the DPE-substituted SAM on a flat substrate, which is close to the length of 11 $-CH_2-$ chains and the DPE group. Thus, the surface density of an ideal DPE monolayer on a flat surface was calculated to be $\sim$2.7 DPE molecules/nm^2. Cyclic voltammetry (CV) measurements on the Au substrate also confirmed the formation of a well-packed monolayer (based on the area of the electrode, electron density, and charge injected).[38] A molecular density value of 24.1 Å^2/molecule was calculated, which is typical of a well-packed SAM monolayer. From batch to batch, the nature of adhesion on Au and Si wafers may lead to different densities of DPE on the surface. Not all SiOH groups on the silica surface can react with the chlorosilane. The steric demands of dimethylchlorosilyl groups and the possibility of silicate polymerization with dichloro- and trichlorosilane derivatives are factors.[39] On the other hand, the thiol-on-Au SAM may be subject to stability issues especially with reaction at higher temperatures.[33]

It is important that all DPE on the Si and Au surfaces is activated by *n*-BuLi (to form a 1,1-diphenylhexyllithium derivative).[34] Thus, excess *n*-BuLi or *s*-BuLi was used. However, this requires removal of the excess BuLi, which can also initiate polymerization. Oosterling and co-workers polymerized styrene from both bound and free initiator without removing the excess and assuming the same MW of grafted and nongrafted polymer.[15] Free initiator can strongly affect polymerization results if the propagation rates are different with surface-bound initiators. We have recently reported the "living" nature of surface-bound DPE for anionic polymerization on nanoparticles by demonstrating a linear relationship between monomer concentration and MW and by monitoring the appearance/disappearance of the red Li−DPE anion complex.[20,21]

Homopolymers and Characterization of Grafted Polymer at the Surface. Using the polymerization procedure outlined, PS homopolymers were prepared. This involved standard vacuum line procedures with degassing and the break-seal approach for anionic polymerization. Polymerization proceeded by introduction of *n*-BuLi and removal of the excess, followed by addition of the monomer. After polymerization, all films were washed for more than 36 h by Soxhlet extraction in toluene prior to characterization of the surfaces. This was necessary to ensure complete removal of any polymers that might have formed in solution (from unattached initiator or *n*-BuLi) and physically adsorbed at the surface. Alternatively, a washing/thickness monitoring procedure was also employed for the Au substrates. No significant difference with this method was observed on Au, as also reported by Ulman et al.[19]

The data in Table 1 indicate *all* attempts made for PS polymerization with various conditions on Si wafers and Au substrates. Immediately noticeable is the large distribution of film thickness and contact angles even with similar concentrations and polymerization conditions, for example, cosolvent and reaction time. The best repeatable attempts with benzene as solvent with THF obtained films of 16.1 ± 0.2 nm average thickness. These measurements are for *dry or glassy* polystyrene brushes as determined by ellipsometry. Also noticeable is that the use of TMEDA additive and Au substrate resulted in a thicker film, 23.4 ± 0.1 nm (angular shift and Fresnel fit as measured by SPS, Figure 8a). These results are comparable to that obtained by Ulman et al. (18 ± 0.2 nm) on Au surfaces[19] and by Quirk et al., using an analogous initiator (9.5 ± 1.2 nm).[18a] Kunz et al. reported thicknesses up to 245 nm on bulk-polymerized polyacrylonitrile brushes using

(33) Ulman, A. *An Introduction to Ultrathin Organic Films*; Academic Press: New York, 1991.
(34) Quirk, R.; Yoo, T.; Lee, Y.; Kim, J.; Lee, B. *Adv. Polym. Sci.* **2000**, *153*, 69.
(35) Wirth, M.; Fairbank, R.; Fatunmbi, H. *Science* **1997**, *275*, 44.
(36) Sauerbrey, G. *Z. Phys.* **1959**, *155*, 206.
(37) Taylor, D.; Morgan, H.; D'Silva, C. *J. Phys. D*: *Appl. Phys.* **1991**, *24*, 1443.
(38) Inaoka, S.; Collard, D. *Langmuir* **1999**, *15*, 3752.
(39) Fadeev, A. Y.; McCarthy, T. J. *Langmuir* **1999**, *15*, 3759.

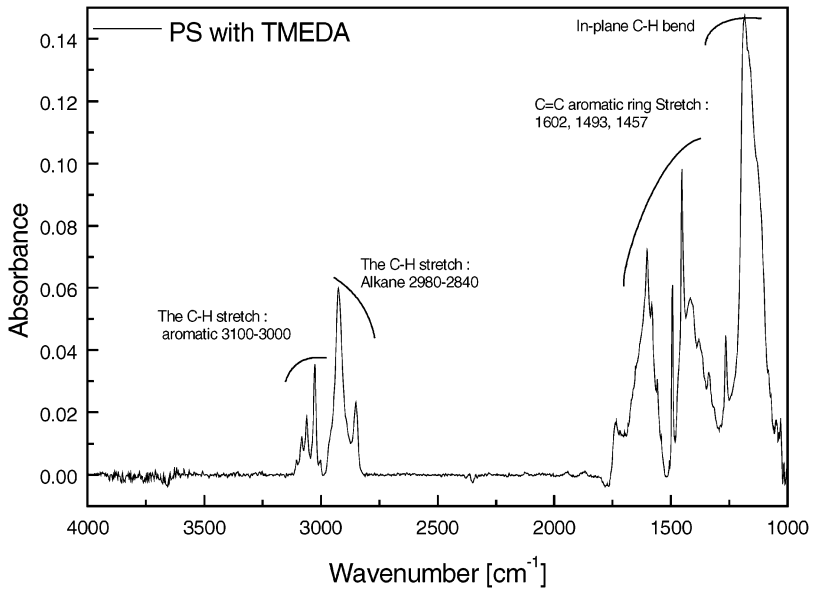

Figure 3. FT-IR spectrum of sample 11 (Table 1, PS in TMEDA solvent) showing relevant peaks typical for PS. The spectrum was taken using PM-IRRAS on Au-coated glass.

lithium di-*tert*-butyl biphenyl on 3-bromopropylsilane SAMs in the presence of 12-crown-4.[18b] Note that the measured thickness can be a function of film swelling. In the case of dry films, the condition is similar to a poor solvent. In a good θ solvent, tethered layers swell. The observed thickness is a balance between osmotic pressure and chain stretching. The osmotic pressure will strongly depend on solvent quality. Recently, Johannsmann et al. demonstrated the swelling behavior of PS brushes in cyclohexane using angle-dependent ellipsometry.[40]

THF was used as a cosolvent for *n*-BuLi in order to accelerate the initiation of DPE. Another attempt used a glovebox procedure with inert atmosphere conditions for polymerization. Again, no significant improvement in thickness was observed as summarized in Table 1. The water contact angle values are generally lower compared to those of bulk polystyrene but comparable to those of previously reported grafted polystyrene brushes of similar thickness.[19] These were verified with hysteresis measurements (advancing and receding) on some samples. Note that contact angles are very sensitive to the topmost surface composition, which changes with factors such as surface energy, surface roughness, and chemical heterogeneity determining the observed value. The large distribution of contact angles and lack of correlation with thickness data or polymerization conditions simply indicate that a variety of surface morphologies, grafting densities, and polymerization efficiencies resulted when using the SiO_x substrate. Also, no correlation can be made with regard to polymerization time and concentration on the wetting properties and thickness of these films. Although several groups have reported thicker films with longer polymerization times, no linear correlation has ever been demonstrated.[18,19] The use of 16% versus 100% DPE (mixed with octadecylsilanes) did not show any clear differences in either contact angle or thickness measurements. Polystyrene was recovered from the reaction solution on some samples (Table 1) where we suspect free BuLi or even cleaved DPE to be present.[13,20]

FT-IR measurements verified the presence of grafted polystyrene based on functional groups present: 3100−3000 cm^{-1}, aromatic or unsaturated CH; 2990−2850 cm^{-1}, aliphatic CH; 1458 and 1496 cm^{-1}, C−C vibrations; and 1506 and 733 cm^{-1}, C═C aromatic stretching vibrations. PM-IRRAS measurements of sample 11 (PS in Au/TMEDA) gave well-defined peaks consistent with a typical PS chemical structure (Figure 3). The spectrum was background-subtracted from absorption of glass (due to a thinner reflecting Au surface, only ∼45 nm).

An important question is, what is the MW and polydispersity index (PDI) of the grafted polymer? In principle, knowledge of these properties correlated with thickness or monomer concentration may give evidence for a living polymerization. Normally, a Poisson distribution is expected for anionic polymerization in solutions.[14,22] As already mentioned, we have observed living anionic polymerization with tethered DPE initiators on silica particle surfaces.[20,21] The red color of particles dispersed in solution (indicating activated DPE) disappeared upon addition of styrene monomer. A linear MW versus monomer concentration trend was observed. However, no direct methods are available for in situ MW determination of polymer brushes on flat surfaces. Ulman et al. estimated a degree of polymerization of $N = 382$ and a grafting density of 7−8 chains/Rg^2 or 3.2−3.6 nm^2/chain based on in situ swelling experiments on an 18 nm thick film as monitored by ellipsometry.[41] Recently, Walker et al. reported MW and PDI values based on the statistical distribution of contour lengths of grafted polymer brushes using AFM.[5a] The values of persistence lengths and other parameters were obtained from fitting force−distance profiles of stretched macromolecules grafted to surfaces. Theoretical predictions have also been used to calculate the MW of polymer brushes grown by SIP on flat surfaces. Wittmer et al. predicted strong differences between polymer molecules grown at surfaces and in solution.[42] In some cases, it can be expected that polymers formed at

(40) Habicht, J.; Schmidt, M.; Rühe, J.; Johannsmann, D. *Langmuir* **1999**, *15*, 2460.

(41) From ref 19, the height h of a brush in a good solvent is given by $h = (12/\pi)^{1/3} N \sigma^{1/3} (\omega/\nu)^{1/3}$, where ω is the excluded volume parameter, approximately $(2\ Å)^3$, N is the number of monomers, and $\nu = (a^2/3)^{-1}$, with $a = 6.7$ Å (the Kuhn length for a polystyrene monomer unit). The polymerization degree can be expressed as $N = [1.074(h_{swollen})^{2/3}]/[h_{dry}(Å^2))^{1/2}]$. When the thickness is 18 nm, the molecular weight calculated from above equation is MW = 39 728 g/mol.

(42) Wittmer, J.; Cates, M.; Jhoner, A.; Turner, M. *Europhys. Lett.* **1996**, *33*, 397.

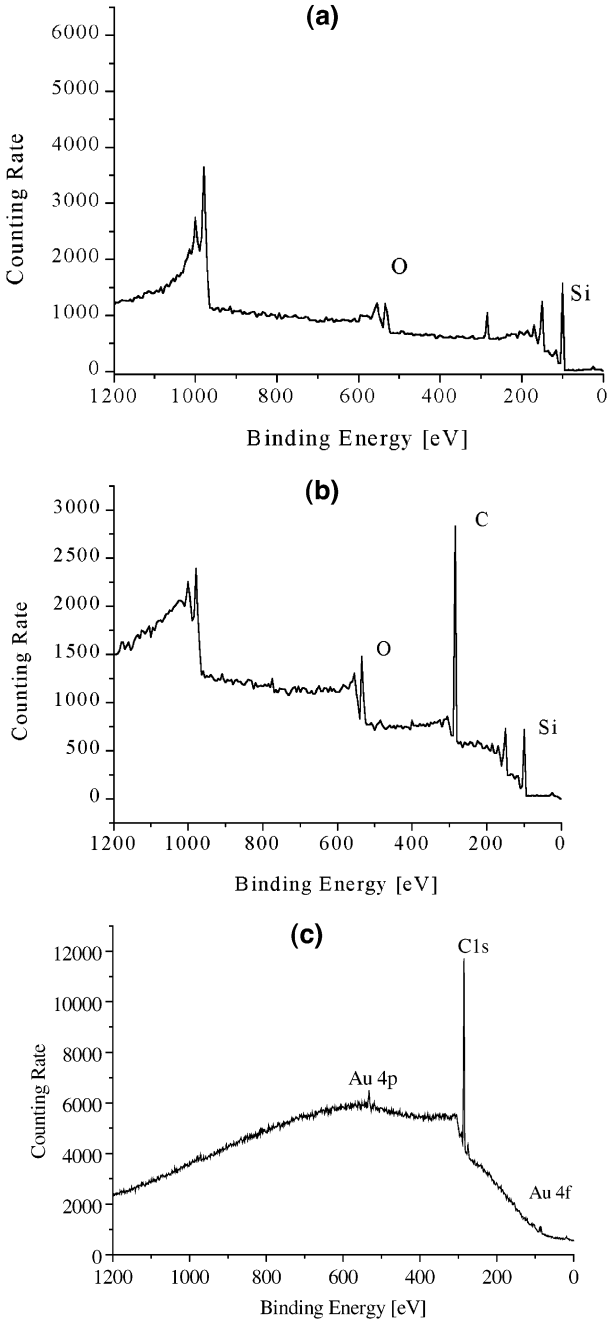

Figure 4. XPS spectra of PS brush formation: (a) SAM of silane−DPE initiators, (b) after polymerization to form PS brushes in benzene/THF (sample 3), and (c) after polymerization to form PS brushes in TMEDA on Au-coated glass (sample 3).

the surface have a much higher PDI compared to those formed in solution. As calculated, long chains are more efficient in reacting with additional monomer than short chains, which consequently grow much more slowly. A basic assumption of this theoretical treatment was that many simultaneously growing (essentially living) chains compete for the *small* influx of monomers to the surface.

XPS spectra showed the relevant C 1s peak (284.5 eV), indicating the presence of PS on the surface (Figure 4b). This peak was absent from the XPS spectra of the Si wafer and was small (by integration) in the spectra of the SAM-coated substrate (Figure 4a). It is interesting to note that the presence of relevant Si peaks (99.8 eV for Si and 103.00 eV for SiO_x), even with the polymerized film, indicates exposure of bare SiO_x surfaces. Also, the Si/O peak ratio is more similar to that in the XPS spectra of the bare Si wafer (not shown). This is consistent with the morphology observed by AFM where the SiO_x surface is exposed by holes (discussed later). The absence of Li peaks (54.9 eV) indicates that no active anion is present and Li^+ cations have been removed by the Soxhlet extraction and washing. The survey scan of the thicker PS in Au/TMEDA films likewise verified the presence of PS brushes on the Au substrate surface (Figure 4c). Note that the ratio of C 1s is much higher with respect to Au (4p and 4f), indicating a thicker brush where the Au surface is barely observed. Also, no Li or other impurities were observed on the spectra.

AFM micrographs were taken from samples with different polymerization conditions (Figure 5). We found that the dry polymer films on SiO_x substrates (measured in ambient air) have a consistent morphology made up of holes, surrounded by reliefs statistically distributed within the domains, as shown in a 3×3 μm scan (Figure 5a). This was found uniformly on all the substrate samples. The smooth relief regions of the film have a root-mean-square (rms) roughness of 0.5−0.8 nm. The depth of the holes corresponds to the thickness of the films.[19] However, at higher resolution scans, an almost dendritic topography was observed for these relief structures (Figure 5b). Branches of the ridges originating from points within the holes can be observed. We believe these to be grafting points of the polystyrene polymer where dewetting from the more polar SiO_x surface is observed. These holes disappear, becoming dimples with thicker films such as the PS in Au/TMEDA. In general, this morphology is uncharacteristic of previously reported grafted PS systems using other types of initiators, in particular with the work by Prucker and Rühe using free radical SIP where they obtained smooth homogeneous and thick films.[43] Ulman et al. also reported homogeneous polymer surfaces with roughness of 0.3−0.5 nm rms.[19] Defects consisting of dense arrangements of dimples or holes (18−20 nm deep) corresponding to the layer thickness were also found. Thus, our observations are more similar to morphologies previously reported by Ulman. However, we would expect lower degrees of polymerization and grafting density for these films on the SiO_x surface.

Again, it should be noted that the morphology of the dry polymer layer is similar to that of films formed in poor solvent conditions.[44] Yeung et al. have analyzed such films using random phase approximation and numerical mean field analysis.[45] For sufficiently poor solvents, they found that laterally homogeneous grafted layers are linearly unstable to fluctuations tangential to the grafting plane. Dimpled surfaces are formed in which the depth and separation of the dimples depend on chain length, solvent quality, and grafting density. This instability is caused by competition of attractive forces between macromolecular chains and grafting constraints. In our case, it is possible that the morphology is caused by dewetting of PS brushes from the more polar SiO_x surface as a consequence of low MW of PS and lower grafting density. Dewetting results from differences in the surface energy (surface tension). A much lower Tg for PS especially at very thin films may also play a role.[49] The morphology is likewise different for the thicker film of PS in Au/TMEDA (23.4 nm with 1.2 nm rms roughness) as shown in Figure 5c. The holes (dimples) are statistically smaller and the relief structures more prominent indicating a higher graft

(43) Prucker, O.; Rühe, J. *Langmuir* **1998**, *14*, 6893−6898.
(44) Luzinov, I.; Minko, S.; Senkovsky, V.; Voronov, A.; Hild, S.; Marti, O.; Wilke, W. *Macromolecules* **1998**, *31*, 3945.
(45) Yeung, C.; Balazs, A. C.; Jasnow, D. *Macromolecules* **1993**, *26*, 1914.

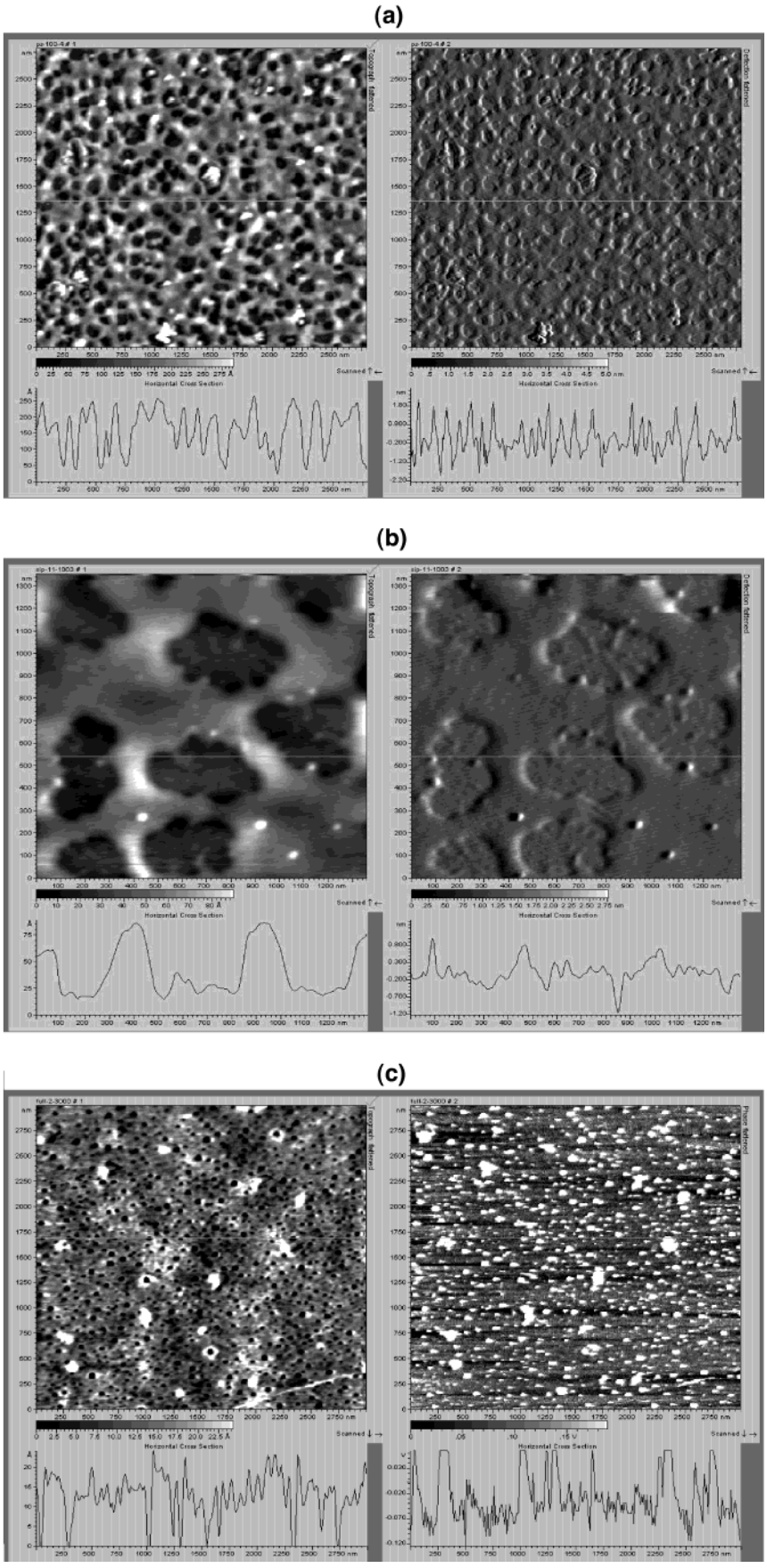

Figure 5. AFM images of the PS brushes. The topological or height image (left) and the amplitude or phase image (right) are shown: (a) after polymerization to form PS brushes in benzene/THF (sample 3), $X-Y$ (3.0 × 3.0 μm) and Z (27.5 nm); (b) small-area scan of PS brushes in benzene/THF (sample 3), $X-Y$ (1.35 × 1.35 μm) and Z (8.5 nm), showing dendritic morphology; and (c) after polymerization to form PS brushes in TMEDA on Au-coated glass, $X-Y$ (3.0 × 3.0 μm) and Z (2.25 nm).

density. Different grafting densities, MW, and PDI affect the conformation of the polymer brush as defined by the Rg and the stretching parameter, γ, normal to the chains' lateral expansion. Recently, Minko et al. have reported the morphology of grafted PS on glass to be dependent on the mechanism of the grafting process, the rinsing procedure, and dewetting from ungrafted polymer.[44] For small and large values of γ, different features of the dimples have been found. At small γ, the layer forms a dimpled surface where the distance between dimples is on the order of Rg and the height of the dimples is on the order of the layer thickness. At large γ, the instability is restricted to a region near to the top of the grafted layer and the distance between the dimples is larger than Rg. Similar behavior for grafted layers has been reported by Tang and Szleifer using scaling analysis.[46] They described three regimes of possible structures: mushrooms, clusters, and layers. Minko et al. have attributed these regimes to different grafting densities based on Rg and thickness.[44]

Although the morphology can be explicitly interpreted, the origin of a lower grafting density is not clear. It can result from a different anionic polymerization mechanism, incomplete initiation, and domain formation after post-polymerization (Soxhlet extraction or solvent washing) treatment. One possibility is removal of "unreacted" initiators after Soxhlet extraction or washing. Another possibility is removal of the silane initiators by *n*-BuLi, during activation of the DPE (the stability of the DPE−silane linkage will need to be investigated, that is, a monochlorosilane vs trichlorosilanes). And perhaps another possibility is the high polarity of the "anionic surface" or the interfacial energy involved, affecting the mechanism of the polymerization.[19]

By polymerization of PS using a more polar additive, TMEDA/benzene, on a Au substrate, these possibilities can be considered. The results as summarized in Table 1 and the XPS, AFM, and IR data can be compared. Under the same high-vacuum conditions used for the synthesis of PS, we obtained a thicker film (23.4 nm) and a higher contact angle at 94° (more characteristic of spin-coated PS), the morphology exhibited smaller dimples (Figure 5c), and XPS revealed a higher ratio for the C 1s peak compared to the Au peaks (Figure 4c). By using a Au substrate, BuLi will not be a factor in possible cleavage of the initiator, since the thiol−Au bond is stable to the anion. The presence of TMEDA, if it is a factor, facilitates polymerization at the interface where the propagating anion end-groups can have a more polar interface and access to monomers.[42]

The latter may be a very important parameter to consider. The changing interfacial properties of propagating living anions increase the polarity and ionophilicity of a growing "polymerization front" at the interface. Note that the interface of a flat surface is composed of a high concentration of growing chain ends confined in a quasi-two-dimensional area.[42] A large difference in surface tension can prevent the flux of monomer (typically nonpolar) at surfaces, creating a more heterogeneous interfacial polymerization mechanism. The role of the solvent molecules and the solvent cage on the propagating anion and Li counterion should be further investigated.[47] A basic assumption of the theoretical treatment by Wittmer was that many simultaneously growing living chains compete for the small influx of monomers to the surface.[42] In this case, the increasing difference between polarities at the interface (ionic) and the nonpolar solution subphase may prevent a homogeneous monomer influx or Fickian diffusion. In effect, the polymerization becomes a self-limiting heterogeneous system preventing formation of inherently high-MW brushes. Also, the presence of free initiators in solution (unremoved excess *n*-BuLi or desorbed initiator) competes with the polymerization of monomers, leaving fewer monomers available for polymerization at the interface and hence resulting in lower MW brushes. This explanation seems to support a general trend for low polymer brush thickness (low MW) with anionic polymerization procedures as reported by others.[18,19] Interestingly enough, the use of a more polar monomer and a crown ether (12-crown-4) resulted in much thicker films.[18b] Important differences should be drawn between anion-free systems such as free-radical polymerization,[7] ATRP,[11] TEMPO,[12] and so forth, where polymer brushes are observed to be much thicker. These SIP protocols do not have ionophilic active centers in their mechanism for propagation. Parallels should be drawn with cationic polymerization methods.[9] Further experiments are being done to look at various monomers, counterions, and solvent combinations and their relationship to any linear trend in polymer brush MW or thickness.

Block Copolymers Grafted from SiO_x and Au Surfaces. Again, using the LASIP procedure, grafted PS-*b*-PI and PBd-*b*-PS block copolymers were prepared. Using silane and thiol−DPE initiators, polymerization was carried out on the SiO_x and Au surface by sequential addition of monomers. For the Au surface, the SAM monolayer formation and polymer formation were also monitored by SPS (Figure 8). Polymerization was carried on a high-vacuum line using custom-designed reaction vessels suitable for sequential monomer introduction (Figure 3). The bound DPE was first activated by addition of *s*-BuLi with subsequent solvent washings (benzene) followed by addition of the first monomer. After this first reaction was allowed to reach completion, the second monomer was added to the living anion and polymerization of the second block was allowed to proceed. Termination was done as in previous cases with methanol addition. Note that the procedure employed is typical of solution procedures for preparing block copolymers except that the substrate with the DPE bound initiator is immersed in monomer solution. Also, for the PBd-*b*-PS brush, the PBd block was attached to the surface first before PS. The schematic diagram for the reaction on Au surfaces and the formation of the block copolymers is shown in Figure 6. The results are summarized in Table 2.

Similar to the homopolymers, fairly thin polymer thicknesses were observed for the copolymers. Ellipsometry results showed dry polymer brush thicknesses on the order of 5−12 nm on Si wafers and Au substrates under similar conditions (benzene, THF as additive). Thus, compared to films prepared by free-radical SIP,[7] the films prepared by anionic polymerization, even for these diblocks, are consistently ultrathin.[18,19]

Again for these block copolymer brushes, the MW and PDI are unknown, much less the actual constitution and volume of the blocks on the polymer brush. From film thickness, the MW of the block copolymer brushes (if it can be obtained) is expected to be low. It will be necessary to prepare grafted polymers from high surface/volume particles in order to obtain more samples for MW and PDI analysis that can be related to thickness.

Nevertheless, the "presence" of the blocks can be confirmed where the sequence of the polymerization procedure ensures consumption of the first monomer followed by polymerization of the second monomer.

(46) Tang, H.; Szleifer, I. *Europhys. Lett.* **1994**, *28*, 19.
(47) Szwarc, M. *Nature* **1956**, *178*, 1168.

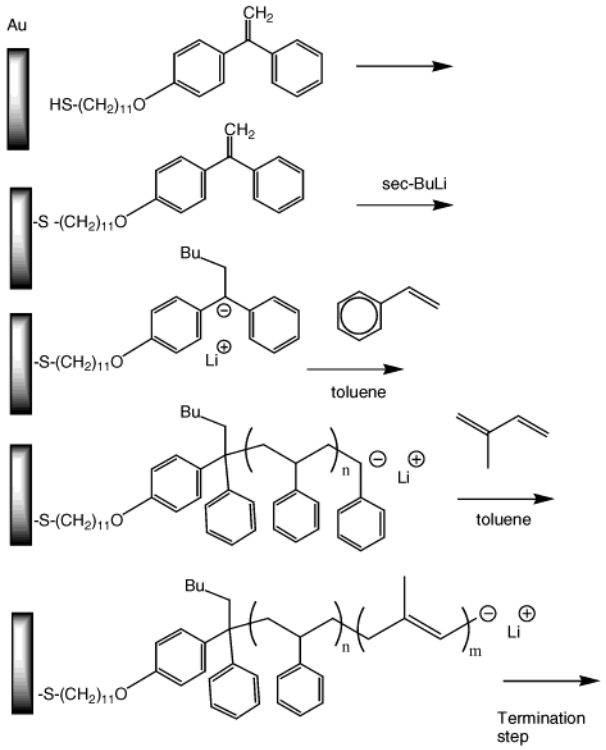

Figure 6. The schematic diagram for block copolymer brush formation on a Au surface.

Table 2. Summary of Thickness and Contact Angle Measurement Results for Block Copolymers[a]

block copolymer sample	thickness/ ellipsometry (nm)	thickness/ SPS (nm)	contact angle (deg)
PS-*b*-PI[b]	6 ± 2 (Au) 8 ± 2 (Si)	5.5 ± 0.1 (Au)	82
PBd-*b*-PS[c,d]	8 ± 2 (Au)	12.0 ± 0.1 (Au)	80

[a] Using benzene/THF as solvent. All polymerizations were done at room temperature, 24−25 °C, with 7 days for the reaction of each monomer block. [b] PS−PI copolymer: 3.6 g of styrene, 5.4 g of isoprene, 2 mL of THF, 5×10^{-3} mol of *s*-BuLi. [c] PBd−PS copolymer: 8.2 g of styrene, 3.6 g of butadiene, 2 mL of THF, 5×10^{-3} mol of *s*-BuLi. [d] The PBd block was attached first to the surface followed by PS.

FT-IR and PM-IRRAS analysis confirmed the presence of PS and PBd blocks polymerized sequentially on the Au surface (Figure 7). The relevant peaks are almost similar to the peaks described earlier (Figure 3) except for the ratio of the peaks at 3100−3000 cm^{-1} for aromatic or unsaturated CH (Ar−CH) and 2990−2850 cm^{-1} for aliphatic CH (Al−CH). In particular, peak area integration results between Ar−CH and Al−CH showed that homopolymer PS has a ratio of 1:4, whereas the block copolymer PBd-*b*-PS has a ratio of 1:18, indicating less aromatic CH vibrations with the PBd-*b*-PS copolymer as expected. The peaks at 1458 and 1496 cm^{-1} for C−C vibrations and at 1506 and 733 cm^{-1} for C═C aromatic stretching vibrations were also observed but at less intensity compared to those for PS in Figure 3. Small peaks at 1650 cm^{-1} were also observed for C═C alkene stretching. These results confirm the presence of PS on the PBd-*b*-PS brush but at a lower volume ratio than in the PS homopolymer.

SPS is highly sensitive for characterizing ultrathin films at the nanometer thickness scale.[48] Combined with other techniques, it is a powerful tool for probing optical and dielectric properties. By monitoring angular-reflectivity changes before and after polymerization, we can obtain information on film formation and optical properties. The resonance angle and shape of the SPS curves are correlated to film thickness and dielectric constants, that is, refractive index. The thickness of these films was calculated based on the Fresnel algorithm fit of the SPS curves. The refractive index used is $n = 1.51$, which is a typical value for these polymers.[49] Figure 8 shows the SPS curves for

(48) Knoll, W. *Annu. Rev. Phys. Chem.* **1998**, *49*, 569.

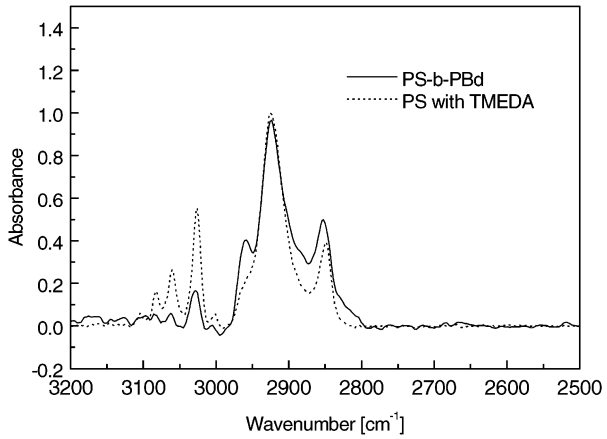

Figure 7. FT-IR spectrum (PM-IRRAS) of the PS-*b*-PBd grafted copolymer compared with that for PS brushes. Note the difference in the ratio between aromatic CH and aliphatic CH between the two grafted polymers.

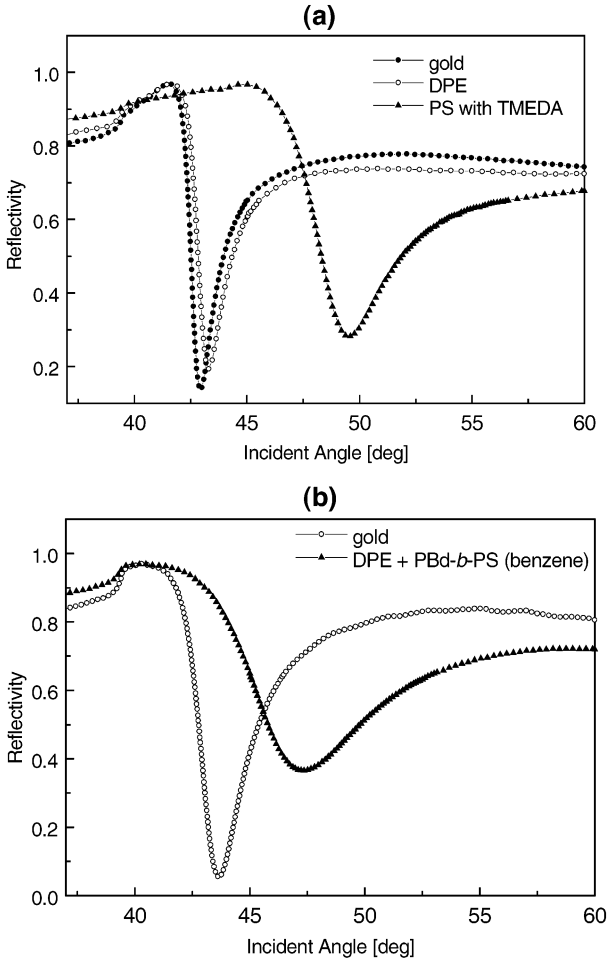

Figure 8. SPS spectra of the (a) PS homopolymer and (b) PBD-*b*-PS copolymer before and after grafting polymerization.

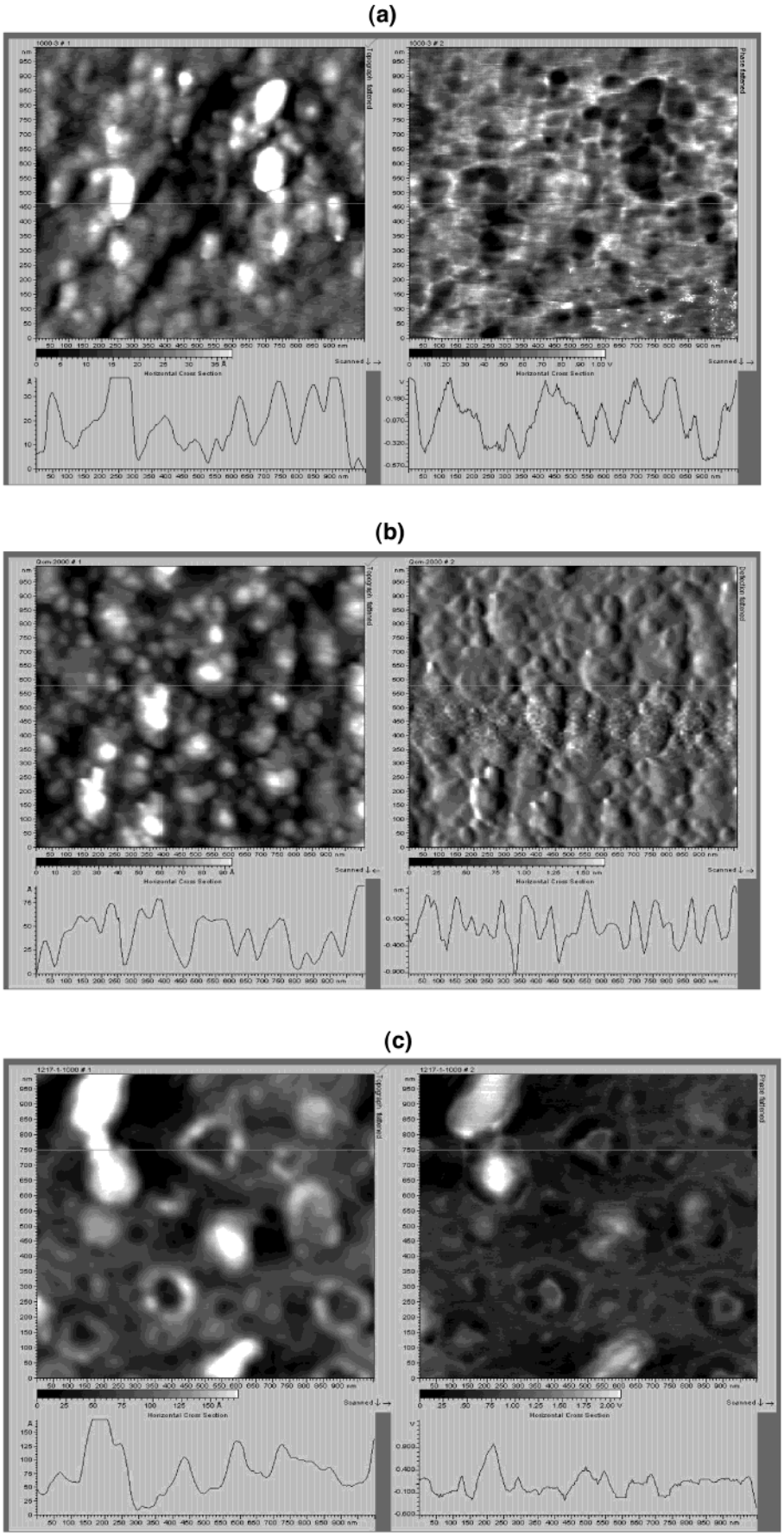

Figure 9. AFM images of the grafted PS-*b*-PBd and PS-*b*-PI copolymers. The topological or height image (left) and the amplitude or phase image (right) are shown: (a) PS-*b*-PBd copolymer on Au-coated glass, $X-Y$ (1.0 × 1.0 μm) and Z (3.75 nm); (b) PS-*b*-PI copolymers on Au-coated glass, $X-Y$ (1.0 × 1.0 μm) and Z (9.25 nm); and (c) PS-*b*-PI copolymers on a Si wafer, $X-Y$ (1.0 × 1.0 μm) and Z (17.5 nm). Note the big difference in morphology between (b) and (c).

PS in TMEDA homopolymer and the PBd-*b*-PS copolymer brush. Immediately noticeable is the smaller angular shift for the PBd-*b*-PS brush consistent with a lower thickness compared to the PS brush. A calculated thickness of 12.0 ± 0.1 nm was obtained for the best PBd-*b*-PS sample using a Fresnel fitting algorithm.[49] Polymerization also resulted in a broadened SPS curve indicating increased inhomogeneity of the films compared to a SAM of the DPE. The broadening of the SPS curve is greater for the PBd-*b*-PS brush compared to the PS brush. The shape and position of the curve are functions of thickness, *d*, and refractive index, *n* (dielectric constant). Broadening of the SPS curve occurs with superposition of SPS curves from multiple resonances.

The films have altogether a different morphology than PS brushes. Noticeable is the absence of holes on PBd-*b*-PS (on a Au substrate), which is characterized by more inhomogeneity in domain structures, increased roughness, and a more globular morphology (1.6 nm rms roughness) (Figure 9). On the basis of the Fourier transform phase (amplitude) image, these domains vary in their phase and depth but are not conclusive for the different block constitutions. The morphology for PS-*b*-PI is different depending on the substrate used for the polymerization process. No holes were observed on PS-*b*-PI on Au, which also exhibited a more globular morphology (2.6 nm total rms roughness). However, PS-*b*-PI on a Si wafer exhibited ring morphologies and holes (5.4 nm total rms roughness), which indicate different depths as revealed in the phase (amplitude) image. Large-area AFM images (3×3 μm) reveal a statistical distribution of these holes almost similar to that of the PS in Si wafer films. This observation is consistent with a substrate-dependent grafting density for polymerization similar to PS homopolymer results. Again, these observed morphologies may be influenced by the wetting (surface tension) and lower Tg properties[49] of polymers at ultrathin films. Also, the sequence for the PBd-*b*-PS brush (PBd grafted to the surface first) may contribute to a different morphology. No regular domain or mesophases were observed as would be expected for bulk thin films for these block copolymers.[27,28] This is perhaps a consequence of the MW difference (lower MW) and interaction parameter differences between the blocks. Selective solvation and annealing may be necessary to observe other morphological features based on surface energy of the blocks.[50,51]

XPS spectra for the PBd-*b*-PS on a Au substrate are shown in Figure 10. The results showed the C 1s peak (284.5 eV), representing the PS and PBd on the film. This peak was absent from the XPS spectra of the Au-coated substrate (not shown). However, Au peaks are prominently present, Au 4p (546 eV) and Au 4d (335 eV), and the ratio of C 1s is lower compared with that of PS in TMEDA in Figure 4c. This is consistent with the low thickness and perhaps low grafting density observed, even though the morphology does not reflect this. Au peaks have a much higher sensitivity factor for photoelectron transitions compared to C (C/Au of 1:17); that is why Au peak intensities are higher compared to the actual constitution.

To verify the presence of the first PBd block on the copolymer, we performed bromination experiments on the

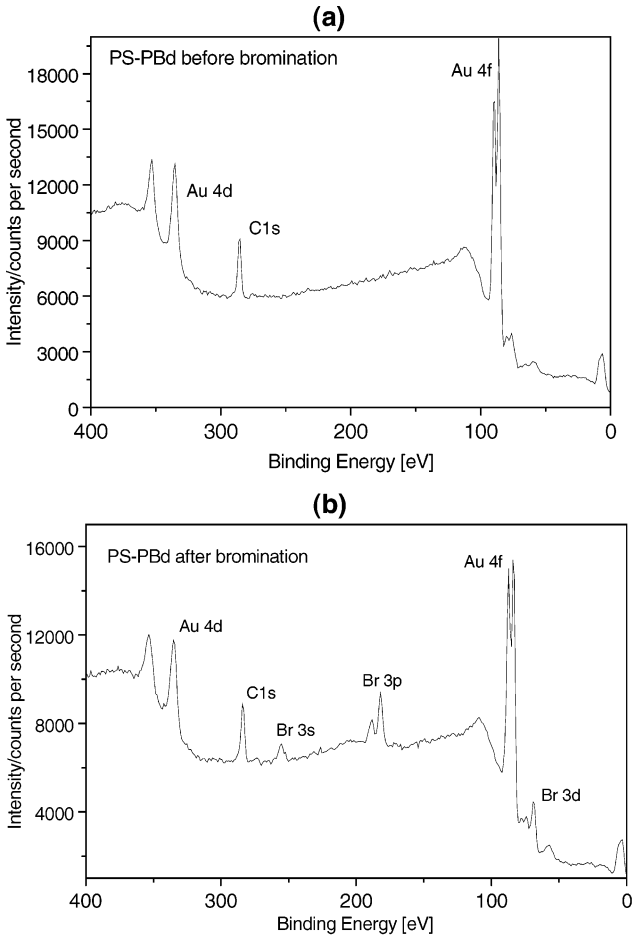

Figure 10. XPS spectra of the PS-*b*-PBd grafted copolymer: (a) before bromination and (b) after bromination.

copolymer brush.[52] If PBd is present, the aliphatic C=C functional groups should be reactive to bromination. In contrast, the aromatic C=C of PS is unreactive. Bromination involved evaporating Br_2 directly on the path of the substrate for a few minutes (sealed chamber). The substrate was then copiously washed with cyclohexane and vacuum oven dried to ensure removal of any unreacted Br_2. The XPS spectra (Figure 10) indicate the presence of the new Br peaks; that is, Br 3s (255 eV), Br $3p_{1/2}$ (188 eV), Br $3p_{3/2}$ (182 eV), Br 3d (69 eV), and Au peaks remained the same. Again Br peaks have a higher sensitivity factor compared to C peaks (C/Br of 1:3). These results confirm the presence of the PBd block on the grafted PBd-*b*-PS brush. We are currently investigating high-resolution XPS scans of the C 1s and Br peaks to possibly distinguish the ratio of the polymer composition with respect to bromination.[53] This may give a relative constitution of the grafted copolymer brush.

In summary, all the results show the presence of the block copolymer by comparison of spectral IR and XPS data and morphology change. In particular, the formation of a block PBd-*b*-PS copolymer brush is confirmed by the sequence of polymerization protocol and spectral data. The presence of the PBd block as shown by XPS and the second PS block as shown by IR confirmed the polymerization of the second monomer (styrene) by the living chain ends of PBd. The sequence of polymerization can allow grafting of only *one polymer block at a time*. In the future,

(49) Prucker, O.; Christian, S.; Bock, H.; Rühe, J.; Frank, C.; Knoll, W. In *Organic Thin Films*; Frank, C., Ed.; American Chemical Society: Washington, DC, 1998; p 233.

(50) (a) Iwata, H.; Hirata, I.; Ikada, Y. *Langmuir* **1997**, *13*, 3063. (b) Zhao, B.; Brittain, W. J. *Macromolecules* **2000**, *33*, 342. (c) Zhao, B.; Brittain, W. J. *Macromolecules* **2000**, *33*, 8813. (d) Zhao, B.; Brittain, W. J.; Zhou, W.; Cheng, S. Z. D. *J. Am. Chem. Soc.* **2000**, *122*, 2407.

(51) Sidorenko, A.; Minko, S.; Schenk-Meuser, K.; Duschner, H.; Stamm, M. *Langmuir* **1999**, *15*, 8349.

(52) Buzdugan, E.; Ghioca, P.; Badea, E.; Serban, S.; Stribeck, N. *Eur. Polym. J.* **1997**, *33*, 1713.

(53) Galuska, A. *Surf. Interface Anal.* **1999**, *27*, 889.

it will be necessary to devise direct methods to probe the properties of grafted block copolymers under optimal conditions for anionic polymerization on surfaces.

Conclusions

This work presents the feasibility of LASIP of homopolymers and block copolymers using a SAM of diphenylethylene derivatives on SiO_x and Au surfaces. A combined approach of spectroscopic and microscopic surface analysis was used to investigate the formation of polymer brushes. FT-IR spectroscopy, XPS, SPS, and ellipsometry confirmed the grafting of the initiator and formation of the polymer film. The results showed polymer brushes with unique morphologies not typical with those of other reported polymer brush systems. These morphologies are determined mostly by the grafting density, MW, and wetting of the polymers. The formation of low-thickness brushes appears to be inherent for anionic polymerization systems where substrate effects and heterogeneity of the growing interface can limit the formation of high-MW polymers. Nevertheless, polymer brushes can be formed and the feasibility of block copolymer formation has been demonstrated.

Acknowledgment. Funding for this project from the Army Research Office (ARO) under DAAD19-99-1-0106 is gratefully acknowledged. We acknowledge Yo Nakamura and Seiji Inaoka for the initiator synthesis and QCM measurements. We acknowledge Dr. Earl Ada and Professor Greg Szulczewski of the Department of Chemistry, University of Alabama at Tuscaloosa, for help with the XPS measurements. We also acknowledge Ramon Colorado and Professor Randy Lee of the University of Houston for PM-IRRAS measurements. Technical support from Molecular Imaging, Maxtek Inc., and Optrel is gratefully appreciated.

LA025962T